Structures of Cys319 Variants and Acetohydroxamate-Inhibited *Klebsiella aerogenes* Urease[†,‡]

Matthew A. Pearson,[§] Linda Overbye Michel,[∥] Robert P. Hausinger,[∥] and P. Andrew Karplus*[,§]

Section of Biochemistry, Molecular and Cell Biology, Cornell University, Ithaca, New York 14853, and Departments of Microbiology and Biochemistry, Michigan State University, East Lansing, Michigan 48824-1101

Received March 6, 1997; Revised Manuscript Received May 5, 1997[⊗]

ABSTRACT: Cys319 is located on a mobile flap covering the active site of *Klebsiella aerogenes* urease but does not play an essential role in catalysis. Four urease variants altered at position C319 range from having high activity (C319A) to no measurable activity (C319Y), indicating Cys is not required at this position, but its presence is highly influential [Martin, P. R., & Hausinger, R. P. (1992) *J. Biol. Chem. 267*, 20024−20027]. Here, we present 2.0 Å resolution crystal structures of C319A, C319S, C319D, and C319Y proteins and the C319A variant inhibited by acetohydroxamic acid. These structures show changes in the hydration of the active site nickel ions and in the position and flexibility of the active site flap. The C319Y protein exhibits an alternate conformation of the flap, explaining its lack of activity. The changes in hydration and conformation suggest that there are suboptimal protein−solvent and protein−protein interactions in the empty urease active site which contribute to urease catalysis. Specifically, we hypothesize that the suboptimal interactions may provide a significant source of substrate binding energy, and such hidden energy may be a common phenomenon for enzymes that contain mobile active site loops and undergo an induced fit. The acetohydroxamic acid-bound structure reveals a chelate interaction similar to those seen in other metalloenzymes and in a small molecule nickel complex. The inhibitor binding mode supports the proposed mode of urea binding. We complement these structural studies with extended functional studies of C319A urease to show that it has enhanced stability and resistance to inhibition by buffers containing nickel ions. The near wild-type activity and enhanced stability of the C319A variant make it useful for further studies of urease structure−function relationships.

Urease (urea amidohydrolase, EC 3.5.1.5) is a nickel-containing metalloenzyme that catalyzes the hydrolysis of urea to form ammonia and carbamate. The resulting carbamate spontaneously decomposes, yielding a second molecule of ammonia and carbonic acid. The hydrolysis of urea has not been observed without the enzyme, so the understanding of the urease catalytic mechanism is an interesting chemical problem. The enzyme is found in many plants, selected fungi, and a wide variety of prokaryotes [reviewed by Hausinger (1993)], where it functions prominently in microbial nitrogen metabolism and is a key virulence factor in certain pathogens [reviewed by Mobley et al. (1995)].

The most well-characterized prokaryotic urease is that from *Klebsiella aerogenes*. The enzyme consists of a 60.3 kDa α-subunit, an 11.7 kDa β-subunit, and an 11.1 kDa γ-subunit (Mulrooney & Hausinger, 1990; Todd & Hausinger, 1987) arranged in a triangle-shaped trimer of trimers [i.e., $(\alpha\beta\gamma)_3$], with three active sites per enzyme (Jabri et al., 1995) (since all residues discussed are located in the α-subunit, the chain designation will be dropped). The active site is in the α-subunit in an $(\alpha/\beta)_8$-barrel domain and contains two nickel ions (Ni^{2+}) located 3.5 Å apart. Ligands of the nickel atoms include four imidazoles (His246 and His272 interact with Ni-1; His134 and His136 interact with Ni-2), Asp360 coordinating Ni-2, a water molecule (originally named Wat-1) that is primarily coordinated by Ni-2, and a bridging carbamylated lysine, Lys217. The electron density for the active site suggested the presence of other water positions (Jabri et al., 1995), and in this work, the model for wild-type urease has been changed to include three water positions. Wat-500 is a metal-bridging ligand. Wat-501 binds to Ni-1, and Wat-502 (formerly Wat-1) binds to Ni-2. Additional residues that are located within the active site and are relevant to the mechanism include His219, Cys319, and His320 (Jabri & Karplus, 1996). Cys319 and His320 are located on a mobile flap that covers the active site.

On the basis of an earlier proposal of Dixon et al. (1980), we propose the following mechanism for urease catalysis. Urea binds with its oxygen coordinated to Ni-1 and accepting a hydrogen bond from His219, which has been implicated in substrate binding by site-directed mutagenesis experiments (Park & Hausinger, 1993b). The urea also accepts a hydrogen bond on one of its amide nitrogens from the side chain of His320, and this interaction, as well as those involving the urea oxygen, polarizes the carbonyl of urea for attack by a hydroxide coordinated to Ni-2, forming a tetrahedral intermediate. As a proton is transferred from His320 to the nitrogen leaving group, this intermediate collapses into ammonia and carbamate, the reaction products (Karplus et al., 1997).

[†] This work was supported in part by USDA Grant 9503443 and by a Hoechst Marion Roussel fellowship to M.A.P.

[‡] The coordinates for all structures have been deposited in the Brookhaven Protein Data Bank with access codes 3kau (wild type), 1fwa (C319A, pH 7.5), 1fwb (C319A, pH 6.5), 1fwc (C319A, pH 8.5), 1fwd (C319A, pH 9.4), 1fwe (C319−AHA complex), 1fwf (C319D), 1fwg (C319S), and 1fwh (C319Y).

* To whom correspondence should be addressed.

[§] Cornell University.

[∥] Michigan State University.

[⊗] Abstract published in *Advance ACS Abstracts,* June 15, 1997.

S0006-2960(97)00514-X CCC: $14.00

Table 1: Data Collection and Refinement Statistics[a]

crystal	unique reflections	completeness (%)	redundancy	R_{sym}[b]	protein atoms	solvent atoms	R_{cryst} (10−2.0 Å)
C319A	51 384	94 (64)[c]	3.3 (2.0)	0.069 (0.279)	5786	281	0.169[d]
C319A (pH 6.5)	52 554	97 (70)	3.4 (2.0)	0.060 (0.250)	5786	281	0.169
C319A (pH 8.5)	53 755	96 (68)	3.3 (2.0)	0.053 (0.259)	5786	281	0.168
C319A (pH 9.4)	52 383	96 (66)	2.8 (2.0)	0.067 (0.312)	5786	281	0.169
C319D	52 745	97 (92)	3.5 (2.3)	0.064 (0.292)	5673	285	0.171
C319S	50 000	92 (59)	2.3 (1.5)	0.056 (0.322)	5786[e]	281	0.176
C319Y	49 732	91 (59)	2.3 (1.6)	0.064 (0.306)	5793	279	0.179
C319A + AHA	52 075	96 (67)	2.3 (1.5)	0.097 (0.395)	5681	277	0.204

[a] All data are for pH 7.5 unless otherwise indicated. [b] $R_{sym} = \sum|I-\langle I\rangle|/\sum\langle I\rangle$, where I is the integrated intensity of a given reflection from Scalepack. [c] All values in parentheses correspond to data in the highest-resolution bin, spanning 2.07−2.00 Å. [d] R_{cryst} for the model with carbonate bound was 0.170. [e] Due to a lack of clear electron density for the side chain of Ser319, this residue was refined as Ala.

Cys319, or its equivalent in other ureases, was initially suggested to be the general acid of urease because its modification by alkylating or disulfide reagents blocked activity (Todd & Hausinger, 1991a,b; Norris & Brocklehurst, 1976; Takishima et al., 1988); however, site-directed mutagenesis studies demonstrated that Cys319 is not essential for catalysis (Martin & Hausinger, 1992). In particular, the C319A, C319S, and C319D variants possessed 48, 4.5, and 0.03% of wild-type activity, whereas the C319Y enzyme was inactive. To examine the role of Cys319 in urease catalysis and to understand the activities of the Cys319 mutants, we have carried out structural studies on these ureases. We have also been able to crystallize the complex of the C319A variant and the competitive inhibitor acetohydroxamic acid (AHA),[1] yielding the first structure of an inhibited urease. Finally, biochemical analyses have shown that the C319A protein has greater stability than the wild-type enzyme and may be preferred for many experiments.

EXPERIMENTAL PROCEDURES

Protein Purification. Ureases were purified from *Escherichia coli* DH5α cells carrying pKAU17 or site-directed mutants of pKAU17, as described by Martin and Hausinger (1992). Protein concentrations were measured by using the Bio-Rad protein assay as described by the manufacturer. Urease activities were assayed at 37 °C in 25 mM HEPES (pH 7.75), 0.5 mM EDTA, and 50 mM urea by measuring the release of ammonia after its conversion to indophenol (Weatherburn, 1967).

Crystallographic Methods. Crystals of the C319A, C319S, C319D, and C319Y ureases were grown as described for the wild-type protein (Jabri et al., 1992). In short, urease crystals of cubic space group $I2_13$ grew in hanging drops equilibrated against 100 mM HEPES (pH 7.5) and 1.5−1.6 M Li_2SO_4. The C319A variant crystals were consistently larger than those for the other variants and for wild-type urease. To determine the C319A structure at various pH values, crystals were soaked for 12−30 h in buffers at pH 6.5, 8.5, or 9.4 prior to data collection. The complex of C319A and AHA was crystallized in a similar manner except the C319A protein sample was incubated for 24 h at 4 °C in the presence of 10 mM AHA prior to crystallization. In an attempt to soak the AHA out of a crystallized complex, one crystal was incubated for 22 h in artificial mother liquor containing no AHA, but data collection revealed that the AHA molecule remained bound to the enzyme with a similar occupancy. All data sets were collected from single crystals at room temperature on an ADSC multiwire area detector system and processed using Scalepack (Otwinowski, 1993). Data collection statistics are in Table 1.

The initial model for C319A urease was constructed starting with the refined coordinates of the wild-type urease at 2.2 Å resolution (Jabri et al., 1995; Protein Data Bank entry 1KAU). Difference electron density maps [[$F_{O(variant)} - F_{C(wild\ type)}$, α_C] and [$2F_{O(variant)} - F_{C(wild\ type)}$, α_C]] were used to determine the position and extent of structural changes. Water molecules were added at difference electron density peaks that were at least $3.0\rho_{rms}$ in $F_O - F_C$ maps and at least $0.5\rho_{rms}$ in $2F_O - F_C$ maps and had good hydrogen bonding geometry. The model was manually adjusted using the program CHAIN (Sack, 1988), and the adjusted model was refined against all data between 10.0 and 2.0 Å by using the conventional positional and restrained individual *B*-factor refinement protocols in X-PLOR (Brünger, 1993), followed by further manual fitting to $2F_O - F_C$ maps. The C319A protein was modeled and refined in two alternate ways: one with three metal-bound water molecules and one with a metal-bound carbonate. The models for the other three C319 variants, the C319A urease at different pH values, and the C319A−AHA complex were refined as above, except that the initial model was the refined model for the C319A protein that included the three metal-bound water positions. For these other variant models, water molecules were added at difference electron density peaks that were at least $4.0\rho_{rms}$ in $F_O - F_C$ maps and at least $1.0\rho_{rms}$ in $2F_O - F_C$ maps and had good hydrogen bonding geometry. In order to determine the relative occupancies for the nickel ions and the metal-bound water molecules in the C319 variants, the *B*-factors were set to 17 for the nickel ions in the Cys319 variant structures (the value observed in the wild-type model) and to 20 for the three water molecules: Wat-500, Wat-501, and Wat-502 (based on the value observed for other atoms ligated to the nickel ions). The occupancies for the nickel ions and the three water molecules were refined using the occupancy refinement protocol of X-PLOR.

Based on the refinements of the C319 variant structures, all with three nickel-bound waters at the active site, the residual density observed at the active site of the wild-type enzyme (Jabri et al., 1995) was reinterpreted as two additional water molecules. Therefore, the wild-type model now contains three metal-bound waters: Wat-500, Wat-501, and Wat-502. The two new water molecules were added to the wild-type model, and the model was subjected to conventional positional refinement in X-PLOR. The *B*-

[1] Abbreviations: AHA, acetohydroxamic acid; HEPES, *N*-(2-hydroxyethyl)piperazine-*N*′-2-ethanesulfonic acid; EDTA, ethylenediaminetetraacetic acid.

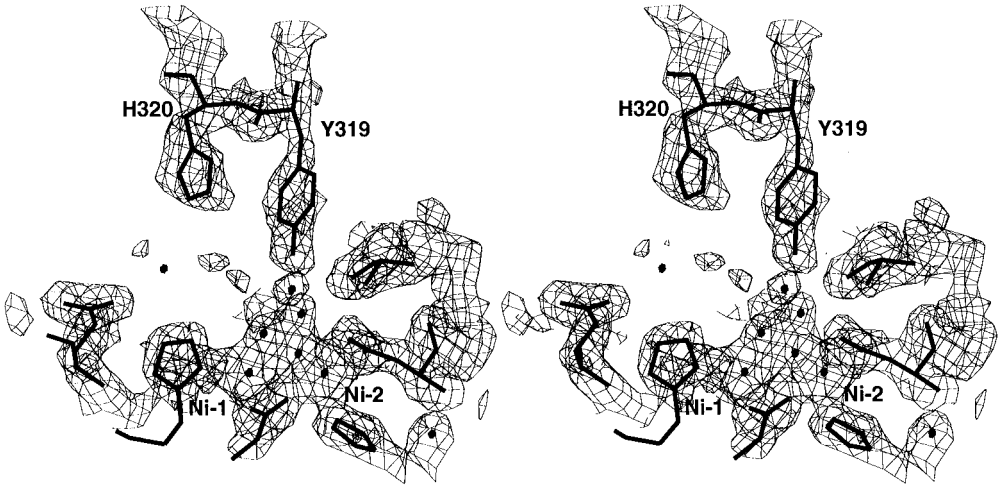

FIGURE 1: Representative electron density for the C319 variant structures. Stereodiagram of the C319Y urease metallocenter and surrounding residues, including Tyr319 and His320. The electron density (calculated with coefficients $2F_O - F_C$ and α_C) is contoured at $1.0\rho_{rms}$.

factors for the nickel-bound water molecules were set to 20 (as in the C319 variants), and their occupancies were refined using the occupancy refinement protocol in X-PLOR

Functional Studies of the C319A Variant. Wild-type and C319A ureases (0.6 mg/mL) were incubated at ambient temperature in sterile 20 mM phosphate buffer (pH 7.4) containing 1 mM EDTA and 1 mM β-mercaptoethanol. Aliquots were assayed weekly for urease activity. Wild-type and C319A ureases were also assayed for urease activity in 25 mM HEPES (pH 7.75) containing 50 mM urea and varying amounts of $NiCl_2$.

RESULTS

Structures of C319 Variant Ureases. Difference Fourier methods were used to determine the crystal structures of C319A, C319D, C319S, and C319Y ureases at 2.0 Å resolution. Each structure has been refined to an *R*-factor of 16−18% (Table 1). In addition, the structure of the C319A species has been determined at pH values of 6.5, 8.5, and 9.4 which span the pH range of enzyme activity, but since the four C319A urease structures show no significant differences, descriptions will refer to the pH 7.5 analysis unless noted. The well-ordered regions of the proteins have electron density that clearly defines their conformations (Figure 1). All of the variant structures are nearly identical to the structure of wild-type urease except for changes in the mobility and position of the active site flap and in the solvent structure surrounding the nickel metallocenter.

(A) Structural Changes of the Active Site Flap. The most apparent structural changes in the C319 variants involve the mobilities (Figure 2) and positions of the residues in the active site flap (residues 312−336). In the wild-type structure, the flap has an average main chain *B*-factor of 38 Å^2, with the peak of disorder at residues 323−325. The C319A species has a similar pattern of mobility with a much lower average main chain *B*-factor of 23 Å^2. In contrast, the other variant structures have a flap that is more flexible than that in wild-type urease. The C319D urease flap is so disordered that residues 317−331 were removed from the model. The C319S urease structure includes the residues of the flap, although they are quite disordered (average main chain *B*-factor = 56 Å^2). In fact, there is no visible density for the side chain oxygen of Ser319, and the residue was

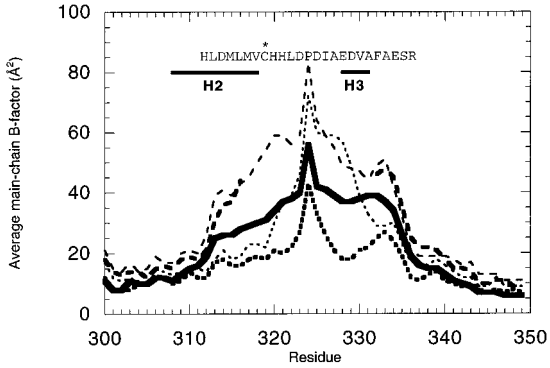

FIGURE 2: Flexibility of the active site flap. The average main chain *B*-factors (Å^2) are plotted for residues 300−350, which includes the mobile active site flap (residues 312−336), in the structures of wild-type (solid line), C319A (thick dotted line), C319D (thick dashed line), C319S (thin dashed line), and C319Y (thin dotted line) ureases. The amino acid sequence is shown for the wild-type urease flap, and Cys319 is indicated with an asterisk. An alignment of urease sequences in this region can be found in Jabri and Karplus (1996; Figure 4). The peak of disorder for all ureases studied is present in a loop that connects α-helices H2 and H3 of the active site flap. Residues 317−331 of the flap have been removed from the model of C319D urease due to a lack of clear electron density, reflecting the increased disorder of this region.

consequently refined as an alanine. The flap of C319Y urease has a different pattern of flexibility than that of the wild-type enzyme; several residues of the flap have main chain *B*-factors lower than those in wild-type urease (*B*-factor = 23 Å^2 for Tyr319), while the remainder of the flap is less well-ordered, with an average main chain *B*-factor of 52 Å^2 for residues 321−330.

In terms of positional variation of mobile flap residues 317−330, both the well-ordered flap in C319A urease (Figure 3A) and the more mobile flap in the C319S protein have conformations that are nearly identical to that found in wild-type urease, with an rms deviation of less than 0.3 Å between C-α atoms of residues 317−330. Shifts in these two variants are focused on residues 332−335 and serve to merge α-helices H3 and H4 of the flap in a manner equivalent to that described for H219A urease and the urease apoenzyme (Jabri & Karplus, 1996). The C319A variant structure contains a new active site water, Wat-270, that is positioned in the pocket created by the loss of the Cys319 Sγ atom and is hydrogen-bonded to Wat-502 and the main

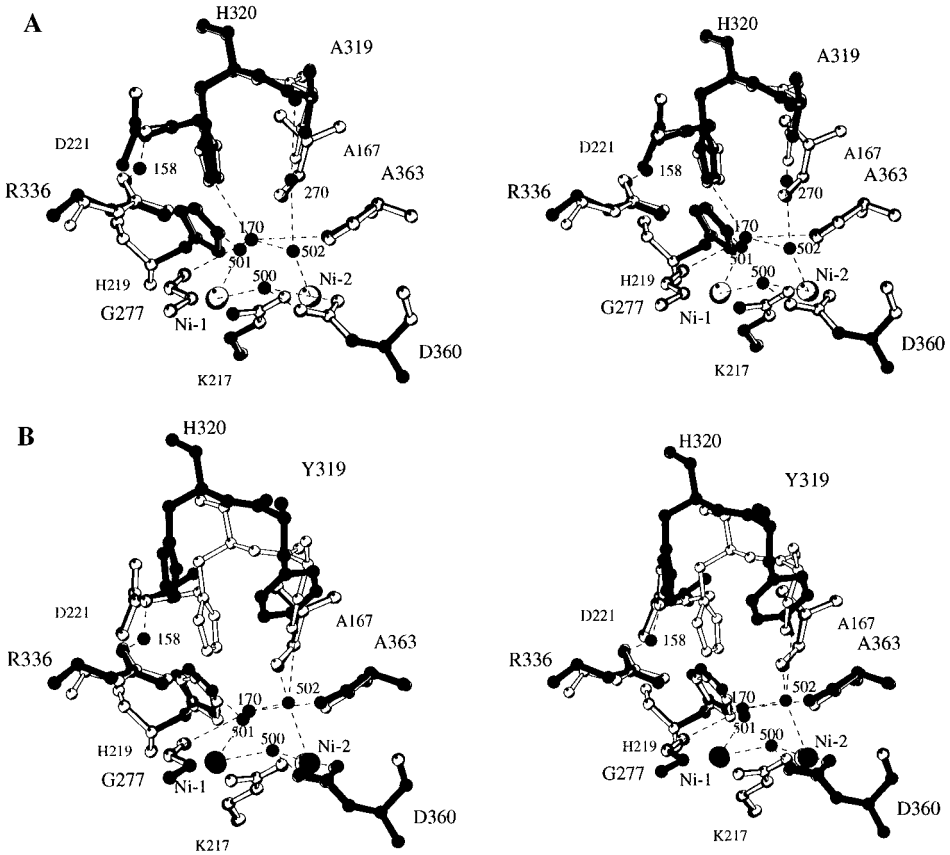

FIGURE 3: Structures of the C319A and C319Y urease metallocenters. (A) Stereodiagram of an overlay of C319A (black) and wild-type (white) ureases. The view is looking at the nickel metallocenter with the carbamylated lysine (K217) behind the metals. Selected metal coordination and hydrogen bonds are shown (dashed lines). No active site residue shifts by more than 0.5 Å. (B) Stereodiagram of an overlay of C319Y (black) and wild-type (white) ureases, with a view similar to that in panel A. Selected metal coordination and hydrogen bonds are shown (dashed lines). There are large shifts in position for residues on the flap, including His320 and Tyr319.

Table 2: Relative Occupancies[a] of Active Site Nickel Ions and Water Molecules[b]

protein	Ni-1 occupancy	Ni-2 occupancy	Ni content[c] (%)	Wat-502 occupancy	Wat-501 occupancy	Wat-500 occupancy
wild-type	1.00	1.00	100	1.25	0.79	0.90
C319A	0.87	0.91	76	1.10[d]	0.82[d]	0.94[d]
C319A (pH 6.5)	0.90	0.94	76	1.01	0.93	1.15
C319A (pH 8.5)	0.89	0.89	76	1.11	0.83	1.05
C319A (pH 9.4)	0.85	0.89	76	1.05	0.89	1.02
C319D	0.67	0.64	54	0.56	0.68	0.70
C319S	0.57	0.57	37	0.75	0.51	0.78
C319Y	0.75	0.73	70	0.98	0.94	1.11

[a] At this resolution, it is not possible to refine the occupancies independently of the *B*-factors, so the occupancies are relative values, based on a refinement with constant *B*-factors. [b] All data are for pH 7.5 unless otherwise indicated. [c] Martin and Hausinger (1992). [d] Refining a carbonate ion in place of the three waters led to an average *B*-factor of 27 Å^2 and occupancies of 1.0 for the four atoms of the carbonate.

chain carbonyl of Ala319. In the C319S protein, Wat-270 is shifted away from Wat-502, and the Ser319 hydroxyl does not extend far enough to replace this hydrogen bond. In contrast to those of the C319A and C319S species, the well-ordered region of the flap in C319Y urease adopts a position very different from that found in the wild-type enzyme (Figure 3B). The side chain hydroxyl of Tyr319 forms a hydrogen bond with Wat-502, and the main chain of the flap is shifted away from the active site. The shift in the positions of residues 312−320 extends α-helix H2 of the mobile flap by two residues and displaces the catalytically important residue His320 by more than 3.5 Å. The positions of flap residues 321−328 are also displaced by up to 6 Å in this variant.

(B) Structural Changes of the Nickel Metallocenter. Changes were observed in the occupancy of the active site nickel ions in the urease structures (Table 2). The refined nickel occupancies determined for each of the four C319 variants were lower than those in wild-type urease, which may partially account for their lower activity, especially for C319D and C319S. The relative occupancies agree reasonably well with the nickel content determined by atomic absorption analysis (Table 2; Martin & Hausinger, 1992).

The electron density surrounding the nickel metallocenter in wild-type urease was initially interpreted as a single water molecule (Wat-1) bound to Ni-2, with residual electron density corresponding to alternate water positions that were not modeled (Jabri et al., 1995). Based on the difference electron density for the C319 variants, this residual electron density was modeled as two additional metal-bound water molecules, and a reexamination of the wild-type electron density led to the inclusion of the same water molecules in the wild-type model. The active site water positions are Wat-500, a water molecule that bridges the nickel ions, Wat-501,

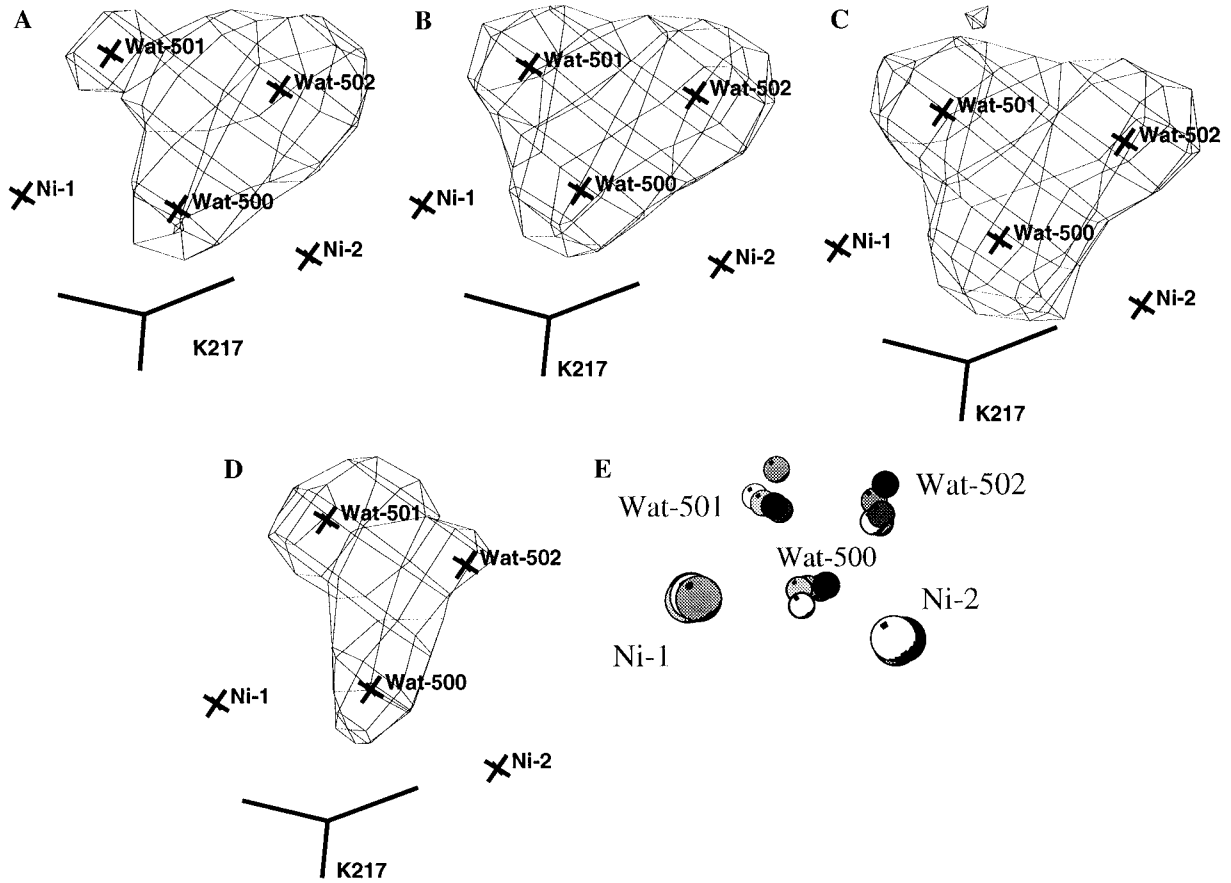

FIGURE 4: Active site water molecules. (A−D) The refined positions of the active site water molecules, Wat-500, Wat-501, and Wat-502, in urease structures are shown along with corresponding difference electron density maps (calculated with coefficients $F_O - F_C$ and α_C with the three water molecules removed from the model) contoured at $4.0\rho_{rms}$. The structures shown are wild-type urease (A), C319A urease at pH 7.5 (B), C319A urease at pH 6.5 (C), and C319D urease (D). (E) Overlay of the active site nickel and water positions for wild-type (white), C319A (pH 7.5) (light gray), C319D (medium gray), C319S (dark gray), and C319Y (black) ureases. The active site water molecules are clustered into three positions: Wat-500, Wat-501, and Wat-502.

which ligates Ni-1, and Wat-502 (formerly known as Wat-1), which ligates Ni-2. The refined distances between the nickel ions and these water oxygens vary from 1.7 to 2.8 Å among the wild-type and C319 variant ureases. These water positions were refined with all interactions between the three water molecules turned off, resulting in interatomic distances between the water oxygen positions that were too short to allow the water molecules to be present simultaneously. For example, these inter-oxygen distances were 2.0−2.5 Å in wild-type urease and 1.9−2.0 Å in C319A urease. However, the strength of the electron density suggested that these positions have nearly full occupancy in these ureases. An alternative interpretation is that this density represents a carbonate ion, as was seen in a recent structure of bovine lens leucine aminopeptidase (Sträter & Lipscomb, 1995). A test refinement carried out for C319A urease with a carbonate in place of the water molecules resulted in a plausible model having an *R*-factor of 17.0%, which is very similar to the value obtained for the model with water molecules. However, while the carbonate model fits the observed electron density, the bond angles for the carbonate−metal interactions are very unfavorable, ranging from 75 to 95°. The identity of the ambiguous density at the nickel center of the wild-type and C319 variant ureases was tentatively assigned to solvent (see Discussion) to allow comparison among these proteins.

Clear differences in the active site solvent structures were observed for the wild-type and C319 variant ureases. For example, in wild-type urease, the electron density corresponding to Wat-502 is stronger than that for the other positions (Figure 4A). This is in contrast to the C319A protein, where the electron density is roughly equivalent for the three positions (Figure 4B). The electron density at these three positions in C319A urease changes very little at lower pH (6.5) and higher pH (8.5 and 9.4) (Figure 4C). In the C319D protein, the electron density is very weak at Wat-502, the predominant position in wild-type urease (Figure 4D). The refined occupancies for the water molecules modeled at these positions also reflect the variation among the wild-type and C319 variant structures (Table 2). Despite the variation in occupancy, an overlay of the C319 mutant and wild-type structures clearly shows that the active site water molecules are clustered in the three "native" positions: Wat-500, Wat-501, and Wat-502 (Figure 4E).

Structure of Acetohydroxamic Acid (AHA) Bound to C319A Urease. In order to elucidate the mode of interaction between a ligand and urease, the structure of AHA bound to C319A urease was determined. In addition, the kinetics of AHA inhibition of C319A urease activity were studied and compared to those observed for the wild-type enzyme. AHA is a slow-binding competitive inhibitor of urease, meaning that the inhibitor forms an initial complex with the enzyme (EI), which slowly becomes a more stable complex (EI*) (Todd & Hausinger, 1989; Morrison & Walsh, 1988). In this situation, the relevant kinetics constants are K_i, k_5, k_6, and K_i*, where K_i is the inhibition constant for formation

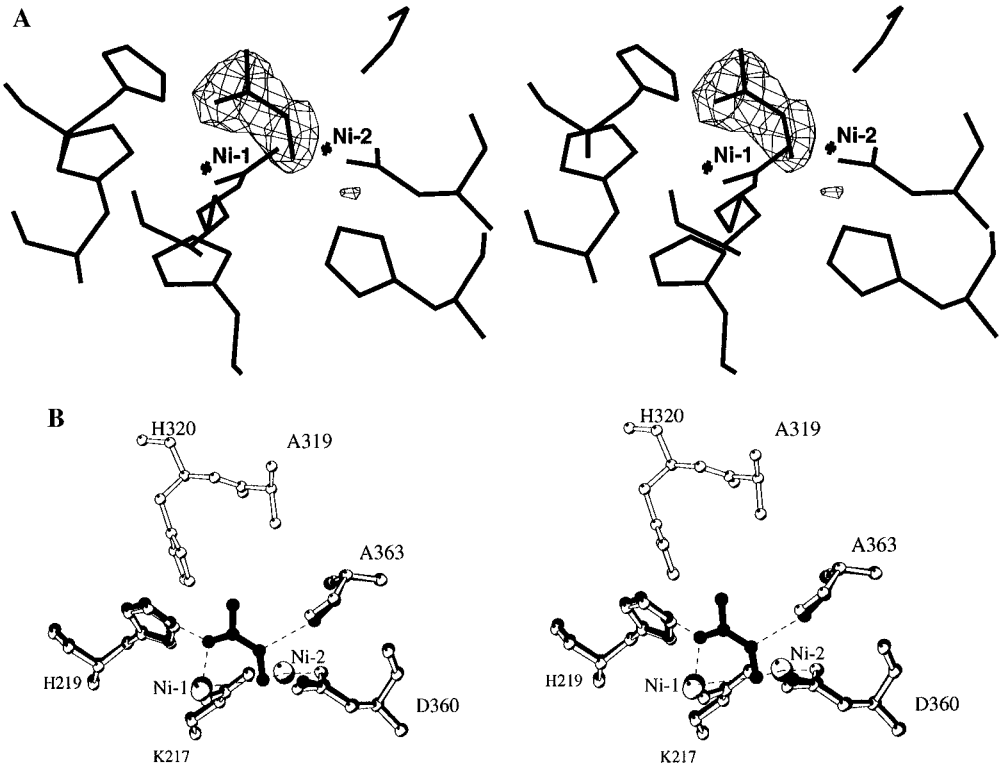

FIGURE 5: Acetohydroxamic acid (AHA) bound to C319A urease. (A) Stereodiagram of the refined structure of AHA bound to C319A urease with difference electron density (calculated with coefficients $F_O - F_C$ and α_C with the AHA molecule removed from the model) contoured at $4.0\rho_{rms}$. (B) Stereodiagram of an overlay of C319A urease bound to AHA (black) and C319A urease alone (white). Metal coordination and hydrogen bonds are shown (dashed lines). The inhibitor coordinates to both metals and makes hydrogen bonds with the side chain of His219 and the main chain carbonyl of Ala363. The disordering of the flap in the AHA-bound structure is indicated by the missing black model for Ala319 and His320.

of the initial EI complex, k_5 and k_6 are respectively the rate constants for forming and dissociating the EI* complex, and K_i* is the overall inhibition constant expressed by Morrison and Walsh (1988) as

$$K_i^* = K_i \frac{k_6}{k_6 + k_5} \quad (1)$$

AHA was found to have kinetic constants for inhibition of soluble C319A urease similar to those for the wild-type enzyme. For wild-type urease, $K_i = 1.4$ mM, $k_5 = 0.047$ s^{-1}, $k_6 = 9.2 \times 10^{-5}$ s^{-1}, and $K_i^* = 2.6$ μM (Todd & Hausinger, 1989); for C319A urease, $K_i = 1.3$ mM, $k_5 = 0.045$ s^{-1}, $k_6 = 8.5 \times 10^{-5}$ s^{-1}, and $K_i^* = 2.5$ μM. Whereas we were not able to soak AHA into crystals or cocrystallize it with wild-type urease, cocrystallization of the complex of AHA and C319A urease was achieved.

Difference electron density maps clearly show the position of AHA in the C319A urease active site (Figure 5A). The structure of the complex was refined at 2.0 Å resolution to an *R*-factor of 20%. AHA is bound to both nickel ions in the active site, with the carbonyl oxygen interacting with Ni-1 and accepting a hydrogen bond from the Nϵ atom of His219, and the other oxygen bridging the nickel ions. This interaction with the metal ions replaces the three water molecules (Wat-500, Wat-501, and Wat-502) which are no longer present. The nitrogen of AHA makes an additional hydrogen bond to the main chain carbonyl oxygen of Ala363. Comparison of the AHA-bound and unliganded structures of C319A urease shows no conformational changes, except that the active site flap becomes sufficiently disordered in the AHA-bound structure that residues 318−331 were not modeled (Figure 5B). The close interaction that would be present between the methyl group of AHA and the Nϵ atom of His320 would be unfavorable and could force the flap away from the active site into a disordered state.

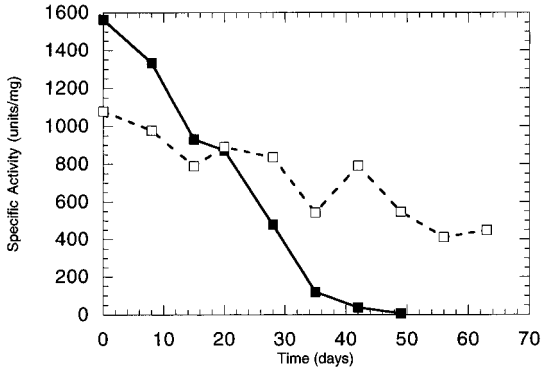

FIGURE 6: Stability of C319A and wild-type ureases. C319A (open squares) and wild-type (closed squares) ureases were incubated at ambient temperature in sterile 20 mM phosphate buffer (pH 7.4) containing 1 mM EDTA and 1 mM β-mercaptoethanol. Aliquots were assayed weekly for urease activity.

Enhanced Stability of C319A Mutant Urease. The C319A urease was shown to be much more stable than the wild-type enzyme during long term storage with β-mercaptoethanol. For example, the C319A species retained nearly half of its activity over 70 days, while wild-type urease lost nearly all of its activity by 50 days (Figure 6). The C319A urease was also found to be inhibited less than wild-type by elevated levels of nickel ion. C319A and wild-type ureases were assayed in buffer containing urea and $NiCl_2$ at various concentrations. Whereas $NiCl_2$ inhibits both ureases, the wild-type enzyme was affected by lower concentrations and

to a greater extent than C319A. For example, K_i values for nickel ion were calculated to be 9.1 μM for C319A urease and 3.2 μM for wild-type urease, and saturating levels of the metal ion (500 μM) resulted in 15 and 7% of the activity remaining, respectively (data not shown). The assays showed that the inhibition of the activity of both ureases by nickel ions was rapid, reversible, and time-independent, indicating that the inhibition was due to the binding of nickel to the enzyme and not due to slow binding or to a reaction, such as disulfide formation, catalyzed by nickel ions.

DISCUSSION

We undertook structural and functional studies of Cys319 variant ureases to better understand the mechanism of urease catalysis. The side chain of Cys319 is not essential, as shown by the remaining activity of C319A urease (Martin & Hausinger, 1992); however, structural comparisons among the C319 variant and wild-type structures reveal crucial elements of urease catalysis, and the structure of AHA bound to the C319A variant has provided informative details about a urease−inhibitor complex.

Interpretation of the Urease Active Site Solvent Structure. The identity of the bound solvent at the nickel metallocenter remains ambiguous. The observed electron density could be interpreted as three water molecules that must be partially occupied due to short inter-oxygen distances or, alternatively, as a carbonate or other trigonal ion, although no such ions were added to the crystallization conditions. Since carbonate may be present (from dissolved carbon dioxide), an alternate refinement of the C319A variant with a carbonate bound was carried out and resulted in a reasonable model. However, since carbonate is not a urease inhibitor (200 mM bicarbonate had no effect on activity, I.-S. Park and R. P. Hausinger, unpublished data), and the carbonate−metal interaction geometry is poor, this interpretation is not compelling. Moreover, a comparison of this electron density between the wild-type and C319 variant enzymes shows that the strengths of the three putative oxygen positions appear to vary independently (Figure 4), as would be more consistent with a group of water molecules. At this point, we have chosen to describe the electron density in terms of water positions. The high refined occupancy for the three water positions that can only be partially occupied suggests that this interpretation is not the complete story. However, the main conclusions of this work do not depend on the exact interpretation but are based only on the fact that solvation structure changes in the variant structures.

Suboptimal Interactions at the Urease Active Site. There are several interactions of residues in the wild-type urease active site flap that appear to be suboptimal. In terms of interactions between protein residues, it has been pointed out by Jabri and Karplus (1996) that the side chain of His320 is in close proximity to the side chains of both Asp221 and Arg336, but the geometry is not optimal for hydrogen bonding between these residues. His320 also appears to accept a hydrogen bond on Nϵ from Wat-170; however, this water also appears to donate hydrogen bonds to two main chain carbonyls. Since this water cannot donate three hydrogen bonds, one of the hydrogen bonds is not formed, and the water's interactions are suboptimal. In this study, we have extended these observations to include suboptimal interactions between the nickel metallocenter and solvent. The active site water molecules (Wat-500, Wat-501, and Wat-502) have inter-oxygen distances that are too short to allow their simultaneous occupancy. Since the ligation spheres of the two nickel ions cannot both be satisfied by multiple water molecules without a large steric penalty, there appears to be competition for water occupancy at the three positions. All of these suboptimal interactions must contribute to the flexibility of the flap by destabilizing the closed conformation. Evidence for this is found in the C319A urease structure. In this variant, removal of the Cys319 Sγ increases the size of the active site cavity, which should relax the constraints on bound solvent and allow for improved protein−solvent interactions. For example, a new water, Wat-270, makes hydrogen bond interactions with the protein and with a nickel-bound water, interactions that are not possible in the more constrained wild-type active site. Importantly, these changes in active site solvation are accompanied by an increase in the order of the flap.

The presence of suboptimal interactions in the urease active site has implications for the catalytic mechanism. An enzyme drives a reaction by decreasing the free energy difference between the initial state, which includes the empty (solvated) enzyme and solvated substrate, and the enzyme−transition state complex. This can be accomplished in one of two ways: by the enzyme binding the transition state in an exceptionally favorable way or by the initial state of solvated enzyme having a higher free energy, possibly through the presence of suboptimal interactions between protein side chains and between the protein and solvent. The suboptimal interactions effectively lead to a greater rate enhancement if they are relieved as the transition state is reached. This occurs even if the interactions that the enzyme makes with the transition state are not especially favorable. The same principle can be used to increase the substrate binding energy. In this case, the suboptimal interactions would be partially optimized as the substrate binds. Thus, the observed suboptimal interactions in the urease active site (between protein residues and between the protein and solvent) could contribute a substantial amount of energy for the binding of both the substrate and the transition state. Indeed, it has been observed that the binding energy of several ligands to proteins includes a favorable enthalpy change due to the reorganization of the solvent upon binding (Chervenak & Toone, 1994; Lemieux, 1996), indicating that the interactions with the solvent were suboptimal The activation of an enzyme through suboptimal interactions is reminiscent of an entatic state, an activated state poised for catalysis (Vallee & Williams, 1968; Williams, 1995). The derivation of binding energy by this process of optimizing suboptimal interactions appears to be possible for any enzyme with flexible active site loops, and it may be a widespread feature of catalysis by such enzymes.

Binding Mode of AHA. The structure of AHA bound to the C319A variant provides the first structural details of ligand binding to the binickel active site of urease and distinguishes between the previous models proposed for hydroxamic acid binding to urease (Todd & Hausinger, 1989). The binding mode of AHA to urease is rather similar to the structure of a hydroxamate bound to the bimagnesium active site of xylose isomerase (Allen et al., 1995), except that in the xylose isomerase structure the carbonyl oxygen is the metal-bridging ligand. The AHA binding mode is remarkably similar to the structure of hydroxamates bound

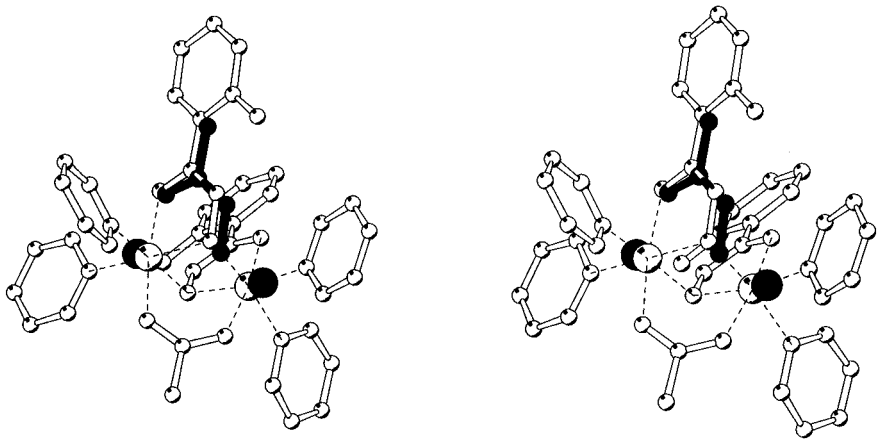

FIGURE 7: Comparison of the C319A−AHA structure to that of a model compound. Stereodiagram of an overlay of the metal and inhibitor structure in C319A−AHA (black) and the structure of $[Ni_2(Hshi)(H_2shi)(pyr)_4(OAc)]$ (white), a compound proposed to model the interaction of hydroxamic acid inhibitors with urease (Stemmler et al., 1995). Metal coordination bonds are shown (dashed lines) for the small molecule structure. The orientations of the hydroxamic acids relative to the metals in the two structures are nearly identical.

to a binickel center in a model compound reported by Stemmler et al. (1995) (Figure 7), corroborating the fact that the synthetic nickel complex was a good model for hydroxamic acid inhibitors bound to urease. The observed AHA binding position provides useful information supporting the proposed roles for active site residues, especially His219 and His320, as discussed below.

Roles of Three Conserved Residues in Catalysis. (A) Cys319. The conserved residue Cys319 was originally proposed to act as a general acid in the hydrolysis of urea, but the activity of C319A urease shows that, in fact, the cysteine side chain is not necessary for catalysis. One reason for determining the structures of the C319 variants was to find structural features that could explain why C319A urease is active, why the C319D and C319S proteins are much less active, and why the C319Y variant has no activity. In the C319A urease, Wat-270 takes approximately the position formerly occupied by the Sγ atom of Cys319, raising the possibility that Cys319 might still be a general acid in wild-type urease, and that Wat-270 carries out this role in the active C319A urease, but not in the other variants. However, the water is not activated by any strong interactions with the protein, and so it would be a much weaker acid than a thiol, which is not consistent with the high activity of the C319A enzyme. Also, Wat-270 is positioned closer to the nickel metallocenter than the Sγ atom of Cys319, and according to the current model for urea binding (Karplus et al., 1997), there will not be room for Wat-270 to bind simultaneously with urea. Since it does not appear possible for Wat-270 to substitute as a catalytic acid, the activity of the C319A urease supports the interpretation that Cys319 is not acting as a general acid catalyst in a rate-limiting step in wild-type urease.

The identity of residue 319 does have an effect on the position of neighboring residues. The C319A structure shows no major shift in any active site residue, including the residues of the flap. This is in sharp contrast to the other three variants which cause the flap to become more disordered (C319D and C319S) or to shift by several angstroms (C319Y). Thus, it appears that one role of residue 319 is to allow its neighboring residues, which may be important for catalysis, to be appropriately positioned in the active site.

(B) His219. Mutagenesis experiments have implicated His219 as being involved in substrate binding (Park & Hausinger, 1993b). In the wild-type urease structure, the Nϵ of His219 donates a hydrogen bond to the partially occupied Wat-501 position, which is also bound to Ni-1. Since His219 accepts a hydrogen bond at Nδ from the main chain nitrogen of Asp221, it is the Nϵ-protonated neutral form of the histidine that donates a hydrogen bond (Jabri & Karplus, 1996). This is consistent with the K_M of urease being relatively independent of pH above a pH of ~5 (Todd & Hausinger, 1987). The position of AHA bound to C319A urease shows that the carbonyl oxygen of AHA, which is analogous to the carbonyl oxygen of urea, binds to Ni-1 and accepts a hydrogen bond from His219. This structure provides further support for the proposed substrate binding site, where urea binds to Ni-1 and His219, putting it in position to be attacked by the hydrolytic water (Wat-502, formerly known as Wat-1).

(C) His320. Mutagenesis and chemical modification experiments have implicated His320 as a crucial residue for catalysis (Park & Hausinger, 1993a,b). The C319A urease has His320 in a position almost identical to that in the wild-type enzyme, consistent with the variant's activity. The activity of C319A urease is lower than that of the wild type, possibly because the flap is more well-ordered (possibly decreasing the available binding energy), because the nickel content is slightly lower, and/or because of small changes in the geometry of substrate binding. The mutation of Cys319 to Asp or Ser causes the flap to become more disordered. The removal of His320, positioned on the flap, from the active site, in addition to the lower nickel content, explains the lower activity of these proteins. The C319Y variant adopts a conformation that removes His320 from the active site even when the flap is in the closed position, which explains the complete lack of activity for this protein.

The pH dependence of activity for wild-type urease and the pK_a of His320 indicate that the protonation state of this residue is important for catalysis (Todd & Hausinger, 1987; Park & Hausinger, 1993a,b). Unfortunately, kinetic methods have not unambiguously determined whether His320 is acting in its protonated form (as a general acid) or in its unprotonated form (as a general base). The pH dependence of activity is consistent with either case (Jencks, 1969; Fersht,

1985). The urease structures, however, provide information about the position of His320, which is useful for determining its role. In the structure of wild-type urease, His320 is not in position to interact with a nickel-bound water and act as a general base. It does appear to be positioned to interact with a urea nitrogen, which is consistent with this residue acting as a general acid. In the structure of AHA bound to C319A urease, the methyl group of the inhibitor is directed toward the flap, where His320 is located, and a comparison of this structure to the unbound structure of C319A shows that the methyl group would come in close contact with the Nϵ atom of His320. If urea binds in a similar way to its analog AHA, then one of the amide nitrogens of urea will be poised to accept a proton from the N-ϵ atom of His320, putting this residue in the correct position to act as a general acid (Karplus et al., 1997).

Stability of C319A Urease. Disulfides are known to inactivate *K. aerogenes* urease, apparently by disulfide exchange with the active site cysteine (Todd & Hausinger, 1991a,b). Similarly, it has been suggested that the slow loss of jack bean urease activity in the presence of β-mercaptoethanol and oxygen was due to the formation of a mixed disulfide involving a thiol located in the active site (Riddles et al., 1983). Since C319A urease lacks the thiol group at the active site, we hypothesized that this protein would maintain higher levels of activity than the wild-type urease during long term storage with β-mercaptoethanol. We have shown that this is the case, since over the course of 50 days the C319A protein maintains half of its activity, while the wild-type enzyme activity is almost completely lost.

Nickel, along with other heavy metal ions, can inhibit urease activity when included in the storage or assay buffers (Argall et al., 1992; Blanchard et al., 1988; Smith et al., 1993). However, as shown by the lack of time-dependent inhibition, this loss of activity is not due to metal-catalyzed disulfide formation. It is likely that this inhibition arises from interactions of the metals with residues such as Cys319 and His320 that are located near the active site and are known from isomorphous replacement studies to bind metal ions (Jabri et al., 1995). We reasoned correctly that the C319A variant may exhibit less affinity for nickel ion compared to wild-type urease and showed that it did exhibit less inhibition by this metal ion. Other residues, perhaps including His320, must also be involved in nickel ion inhibition since the C319A variant is still somewhat inhibited.

Due to the high activity, unperturbed structure, better crystallizability, greater longevity, and resistance to inhibition by heavy metals of the C319A urease, we suggest that it is reasonable to use C319A urease in place of wild-type urease in further studies of urease structure−function relations.

ACKNOWLEDGMENT

We thank Evelyn Jabri for growing the first crystals of C319A urease.

REFERENCES

Allen, K. N., Lavie, A., Petsko, G. A., & Ringe, D. (1995) *Biochemistry 34*, 3742−3749.

Argall, M. E., Smith, G. D., Stamford, N. P. J., & Youens, B. N. (1992) *Biochem. Int. 27*, 1027−1036.

Blanchard, A., Razin, S., Kenny, G. E., & Barile, M. F. (1988) *J. Bacteriol. 170*, 2692−2697.

Brünger, A. T. (1993) *X-PLOR*, Version 3.0, Yale University Press, New Haven, CT.

Chervenak, M. C., & Toone, E. J. (1994) *J. Am. Chem. Soc. 116*, 10533−10539.

Dixon, N. E., Riddles, P. W., Gazzola, C., Blakeley, R. L., & Zerner, B. (1980) *Can. J. Biochem. 58*, 1335−1344.

Fersht, A. (1985) in *Enzyme Structure and Mechanism*, p 90, W. H. Freeman & Co., New York.

Hausinger, R. P. (1993) Urease, in *Biochemistry of Nickel*, pp 23−57, Plenum Press, New York.

Jabri, E., & Karplus, P. A. (1996) *Biochemistry 35*, 10616−10626.

Jabri, E., Lee, M. H., Hausinger, R. P., & Karplus, P. A. (1992) *J. Mol. Biol. 227*, 934−937.

Jabri, E., Carr, M. B., Hausinger, R. P., & Karplus, P. A. (1995) *Science 268*, 998−1004.

Jencks, W. P. (1969) in *Catalysis in Chemistry and Enzymology*, pp 182−199, McGraw-Hill, New York.

Karplus, P. A., Pearson, M. A., & Hausinger, R. P. (1997) *Acc. Chem. Res.* (in press).

Lemieux, R. U. (1996) *Acc. Chem. Res. 29*, 373−380.

Martin, P. R., & Hausinger, R. P. (1992) *J. Biol. Chem. 267*, 20024−20027.

Mobley, H. L. T., Island, M. D., & Hausinger, R. P. (1995) *Microbiol. Rev. 59*, 451−480.

Morrison, J. F., & Walsh, C. T. (1988) *Adv. Enzymol. 61*, 201−301.

Mulrooney, S. B., & Hausinger, R. P. (1990) *J. Bacteriol. 172*, 5837−5843.

Norris, R., & Brocklehurst, K. (1976) *Biochem. J. 159*, 245−257.

Otwinowski, Z. (1993) in *Data Collection and Processing* (Sawyer, L., Isaacs, N., & Bailey, S. S., Eds.) pp 55−62, SERC Daresbury Laboratory, Warrington, U.K.

Park, I.-S., & Hausinger, R. P. (1993a) *J. Protein Chem. 12*, 51−56.

Park, I.-S., & Hausinger, R. P. (1993b) *Protein Sci. 2*, 1034−1041.

Park, I.-S., & Hausinger, R. P. (1996) *Biochemistry 35*, 5345−5352.

Park, I.-S., Michel, L. O., Pearson, M. A., Jabri, E., Karplus, P. A., Wang, S., Dong, J., Scott, R. A., Koehler, B. P., Johnson, M. K., & Hausinger, R. P. (1996) *J. Biol. Chem. 271*, 18632−18637.

Riddles, P. W., Andrews, R. K., Blakeley, R. L., & Zerner, B. (1983) *Biochim. Biophys. Acta 743*, 115−120.

Sack, J. S. (1988) *J. Mol. Graphics 6*, 224−225.

Smith, P. T., King, A. D., Jr., & Goodman, N. (1993) *J. Gen. Microbiol. 139*, 957−962.

Stemmler, A. J., Kampf, J. W., Kirk, M. L., & Pecoraro, V. L. (1995) *J. Am. Chem. Soc. 117*, 6368.

Sträter, N., & Lipscomb, W. N. (1995) *Biochemistry 34*, 14792−14800.

Takishima, K., Suga, T., & Mamiya, G. (1988) *Eur. J. Biochem. 175*, 151−165.

Todd, M. J., & Hausinger, R. P. (1987) *J. Biol. Chem. 262*, 5963−5967.

Todd, M. J., & Hausinger, R. P. (1989) *J. Biol. Chem. 264*, 15835−15842.

Todd, M. J., & Hausinger, R. P. (1991a) *J. Biol. Chem. 266*, 10260−10267.

Todd, M. J., & Hausinger, R. P. (1991b) *J. Biol. Chem. 266*, 24327−24331.

Vallee, B. L., & Williams, R. J. P. (1968) *Proc. Natl. Acad. Sci. U.S.A. 59*, 498−505.

Weatherburn, M. W. (1967) *Anal. Chem. 39*, 971−974.

Williams, R. J. P. (1995) *Eur. J. Biochem. 234*, 363−381.

BI970514J